

F.A. Amirli¹ , R.F. Khankishiyeva^{1,2,3,4} , A.F. Mammadova^{1*} ,
S.T. Bayramova¹ , G.G. Azizova¹ , K.B. Irvanlı¹ 

¹Azerbaijan State Oil and Industry University, Baku, Azerbaijan

²Institute of Radiation Problems, Baku, Azerbaijan

³Azerbaijan University of Architecture and Construction Baku, Azerbaijan

⁴Scientific-Research Institute Geotechnological Problems of Oil, Gas and Chemistry, Baku, Azerbaijan

*e-mail: aynur.memmedova@asoiu.edu.az

(Received 9 December 2025; received in revised form 23 December 2025; accepted 25 December 2025)

Reactive compatibilization of EPDM/PA6 blends with dicumyl peroxide: structure–property relationships

Abstract. In this study, binary blends based on ethylene–propylene–diene rubber (EPDM) and polyamide-6 (PA6) were systematically prepared with varying PA6 contents ranging from 10 to 40 phr. Dicumyl peroxide (DCP) was employed as a reactive compatibilizer in order to promote chemical linkages between the elastomeric and thermoplastic components and thereby enhance interfacial adhesion. The blending process was carried out in a Banbury internal mixer under controlled temperature and shear conditions, ensuring homogeneous distribution of the polyamide phase within the EPDM matrix, and the obtained compounds were subsequently compression molded to produce uniform test specimens.

The effect of increasing PA6 concentration on the physicomechanical, thermal, and morphological characteristics of the blends was extensively investigated. Tensile testing demonstrated that the incorporation of higher amounts of PA6 significantly increased tensile strength, modulus, and Shore hardness, which can be attributed to the reinforcing action of the rigid polyamide domains and the formation of peroxide-induced covalent interfacial linkages. Thermal gravimetric analysis further revealed an improvement in thermal stability with rising PA6 content, while differential scanning calorimetry and dynamic mechanical analysis indicated a gradual upward shift in storage modulus and in the glass transition behavior, consistent with the contribution of the stiff thermoplastic phase.

On the other hand, elongation at break and overall elasticity decreased as the PA6 fraction was raised, reflecting the stiffer and less deformable nature of the dispersed polyamide particles. Scanning electron microscopy (SEM) images confirmed that optimal phase dispersion and strong interfacial adhesion were obtained in blends containing approximately 20–30 phr PA6 together with 1.0–1.2 phr DCP. These particular formulations offered the best balance between mechanical strength, flexibility, and heat resistance. Overall, the results demonstrate that peroxide-compatibilized EPDM/PA6 blends possess tunable and application-oriented properties suitable for engineering uses where both mechanical robustness and thermal durability are simultaneously required.

Keywords: EPDM, PA6, reactive compatibilization, dicumyl peroxide, mechanical properties, thermal stability, morphology.

Introduction

Elastomer/thermoplastic blends have attracted significant interest because they combine the elasticity of rubbers with the rigidity and thermal stability of thermoplastics, resulting in balanced performance properties [1–3]. These hybrid systems provide tunable mechanical and thermal behavior and are widely applied in automotive parts, cable insulation, construction, and various engineering devices [4–6].

Ethylene–propylene–diene rubber (EPDM) is a widely used nonpolar elastomer, valued for its resistance to ozone, weathering, and chemicals, as well as its high elasticity and low glass transition temperature [7,8]. However, its relatively low stiffness and tensile strength restrict its application in engineering fields that require enhanced mechanical performance [9]. To overcome these limitations, EPDM is often blended with rigid thermoplastics.

Polyamide-6 (PA6) is a semi-crystalline thermoplastic that exhibits high tensile strength, modulus,

thermal stability, and excellent oil and abrasion resistance [10]. Incorporating PA6 into EPDM increases stiffness and strength while maintaining some elasticity [11]. However, the fundamental challenge arises from their incompatibility: EPDM is nonpolar, whereas PA6 is strongly polar, leading to poor interfacial adhesion, phase separation, and reduced mechanical performance [12,13].

Compatibilization strategies have therefore been widely explored. Maleic anhydride–grafted polymers, such as EPDM-g-MA and SEBS-g-MA, can create covalent bonds at the interface and improve adhesion [14,15]. Despite their effectiveness, these compatibilizers present disadvantages, including high cost, additional synthesis steps, and limited stability under certain conditions [16]. An alternative and cost-effective approach is reactive compatibilization using peroxides.

Dicumyl peroxide (DCP) has been reported as an efficient compatibilizer for EPDM/PA6 blends [17]. Upon decomposition, DCP generates free radicals that promote crosslinking in the EPDM phase and grafting reactions at the EPDM/PA6 interface [18]. This improves phase dispersion, tensile strength, and thermal resistance, although excessive peroxide content can reduce flexibility [19,20].

Previous studies have shown that increasing PA6 loading enhances modulus and tensile strength but reduces elongation at break and overall elasticity [21,22]. Some reports indicate that intermediate PA6 contents (20–30 phr) provide an optimal compromise between strength and elasticity [23]. Morphological studies further confirm that DCP improves phase dispersion and interfacial bonding compared to uncompatibilized blends [24].

Research gap and aim of the study: Although progress has been made, most studies have focused either on maleic anhydride–based compatibilizers or on limited peroxide dosages, leaving open questions about the systematic effect of DCP across a wide PA6 concentration range. The present work addresses this gap by preparing EPDM/PA6 blends with 10–40 phr PA6, compatibilized with DCP, and investigating their mechanical, thermal, and morphological properties. The aim is to identify compositions that achieve an optimal balance between strength, elasticity, and thermal stability, while offering practical insights for industrial polymer blend design.

Materials and methods

For this investigation, commercially available ethylene–propylene–diene rubber (EPDM) (Keltan®

4450, DSM Elastomers, Netherlands) was selected as the elastomeric matrix. This grade contains 50 wt.% ethylene and 5.2 wt.% ENB, which ensures good elasticity and processability. Polyamide-6 (PA6) (Ultramid® B27, BASF, Germany) with a relative viscosity of 2.7 (96% H₂SO₄ solution) was used as the thermoplastic component owing to its high stiffness and thermal stability. Dicumyl peroxide (DCP) (Perkadox® BC-40, Akzo Nobel, Netherlands, 40% active content) was employed both as a crosslinking agent and a reactive compatibilizer, enabling radical-induced grafting at the EPDM/PA6 interface.

Formulation of Blends

The compositions of the blends were defined on a phr basis (parts per hundred parts of rubber), with EPDM fixed at 100 phr (Table 1). To systematically investigate the influence of PA6 loading, its content was varied from 10 to 40 phr, while DCP was introduced at 1.0–1.2 phr. The selected range was based on preliminary trials, which indicated that lower PA6 loadings had negligible reinforcing effects, whereas very high loadings compromised elasticity.

Table 1 – Formulation of EPDM/PA6 blends

Sample Code	EPDM (phr)	PA6 (phr)	DCP (phr)
E10	100	10	1.0
E20	100	20	1.0
E30	100	30	1.2
E40	100	40	1.2

Blend Preparation

The compounding was carried out using a Banbury internal mixer (Haake Rheomix, 160 mL chamber). The mixing parameters were optimized to promote sufficient dispersion of PA6 within the EPDM matrix and to activate the peroxide without excessive degradation. The chamber temperature was maintained at 180°C, with a rotor speed of 60 rpm, and a total mixing time of 8 minutes.

The mixing procedure was as follows:

EPDM was first masticated for 2 minutes to reduce its viscosity and improve incorporation of the thermoplastic phase.

PA6 was then gradually introduced to the chamber to avoid agglomeration and ensure uniform distribution.

Finally, DCP was added to initiate in-situ compatibilization through peroxide decomposition and radical generation.

The compounded materials were subsequently passed through a two-roll mill (Polymix 150L, Germany) at 70°C to obtain uniform sheets. This step was crucial to eliminate unmixed domains and to prepare samples suitable for molding.

Molding and Curing

Test specimens were produced by compression molding using a Carver laboratory hot press. The molding was conducted at 190°C under a pressure of 10 MPa for 15 minutes, conditions chosen to balance peroxide crosslinking with thermoplastic flow. Following molding, the sheets were cooled to ambient temperature under natural air circulation. Dumb-bell-shaped specimens were cut according to ASTM D412 for mechanical testing.

To comprehensively evaluate the blends, a multi-method characterization approach was employed:

Mechanical Properties: Tensile strength, elongation at break, and modulus were measured according to ASTM D412 using an Instron 3365 universal testing machine at a crosshead speed of 500 mm/min. Hardness was determined with a Shore A durometer (ASTM D2240). These tests were performed to quantify reinforcement effects of PA6 and the efficiency of peroxide compatibilization.

Thermal Stability (TGA): Thermogravimetric analysis was conducted on a TA Q50 in a nitrogen atmosphere, heating from 30 to 700°C at 10°C/min. The degradation onset temperature ($T_{10\%}$) and maximum decomposition temperature (T_{\max}) were used to assess improvements in thermal resistance imparted by PA6.

Dynamic Mechanical Analysis (DMA): Performed on a TA Q800 in tensile mode from -100°C to 100°C, at a heating rate of 3°C/min and a frequency of 1 Hz. The storage modulus (E') and $\tan \delta$ curves were analyzed to understand viscoelastic behavior and interfacial bonding.

Morphology (SEM): Fractured tensile specimens were sputter-coated with gold and observed under SEM (JEOL JSM-6610LV, 15 kV). This analysis was essential to correlate mechanical performance with phase morphology and to visually confirm the effectiveness of DCP-induced compatibilization.

Results and discussion

The mechanical performance of the EPDM/PA6 blends compatibilized with DCP is summarized in Table 2.

Table 2 – Mechanical properties of EPDM/PA6 blends

Sample	PA6 (phr)	Tensile Strength (MPa)	Elongation at Break (%)	Modulus (MPa)	Hardness (Shore A)
E10	10	9.8	280	3.5	64
E20	20	13.6	240	5.2	68
E30	30	15.2	210	6.0	72
E40	40	16.0	180	7.3	76

The results clearly demonstrate a progressive increase in tensile strength, modulus, and hardness with increasing PA6 content. This behavior can be attributed to the reinforcing effect of PA6 domains, which restrict EPDM chain mobility and improve stiffness. At the same time, elongation at break decreases, reflecting reduced flexibility due to higher thermoplastic loading.

The optimum balance was achieved for 20–30 phr PA6 (E20, E30), where tensile strength improved significantly while maintaining moderate elasticity. Similar observations have been reported in literature, where intermediate PA6 levels provided a compromise between toughness and stiffness [21–23].

Thermogravimetric analysis results are presented in Table 3.

Table 3 – TGA results of EPDM/PA6 blends

Sample	PA6 (phr)	$T_{10\%}$ (°C)	T_{\max} (°C)	Residue at 700°C (%)
E10	10	328	460	2.8
E20	20	336	468	3.2
E30	30	343	474	3.5
E40	40	350	480	4.0

The onset of degradation ($T_{10\%}$) increased from 328°C (E10) to 350°C (E40), indicating that PA6 improves thermal stability. The maximum degradation temperature (T_{\max}) also shifted positively, which suggests stronger interfacial bonding due to peroxide-

induced compatibilization. The higher char residue at elevated PA6 loadings is consistent with the inherently stable aromatic structure of PA6.

Thus, incorporation of PA6 not only reinforces mechanical properties but also delays thermal decomposition, enhancing the suitability of these blends for engineering applications where heat resistance is critical.

DMA analysis further supports the reinforcing effect of PA6 (Table 4).

Table 4 – DMA parameters of EPDM/PA6 blends

Sample	PA6 (phr)	Storage Modulus E' (25°C, MPa)	T_g (°C, $\tan\delta$ peak)
E10	10	12.5	-61
E20	20	18.2	-58
E30	30	22.7	-55
E40	40	26.5	-52

The storage modulus (E') increased steadily with PA6 loading, confirming enhanced stiffness and restricted chain mobility. Moreover, the glass transition temperature (T_g) shifted from -61°C to -52°C as PA6 content increased, which reflects improved interfacial adhesion and constrained segmental motion of EPDM chains.

The broadening and slight reduction in $\tan\delta$ peak intensity at higher PA6 loadings indicate that DCP-mediated compatibilization effectively reduced interfacial friction, leading to improved stress transfer across phases [22–28].

SEM micrographs of the fractured surfaces revealed distinct differences in phase dispersion depending on PA6 loading. At low PA6 contents (E10), relatively large and poorly adhered PA6 domains were observed. However, with the incorporation of DCP, the morphology significantly improved, especially at 20–30 phr PA6, where finer and more homogeneous dispersion was evident.

At higher PA6 loadings (E40), partial agglomeration and rigid particle domains were visible, which explains the reduced elongation at break despite improved tensile strength. These observations confirm that DCP-induced grafting reactions enhanced compatibility between the nonpolar EPDM matrix and polar PA6 phase.

The graph demonstrates (Fig.1) that tensile strength increases markedly with higher PA6 load-

ings, which can be attributed to the reinforcing effect of the rigid thermoplastic domains restricting the mobility of EPDM chains. In contrast, elongation at break decreases progressively, reflecting the loss of flexibility as the blends become stiffer.

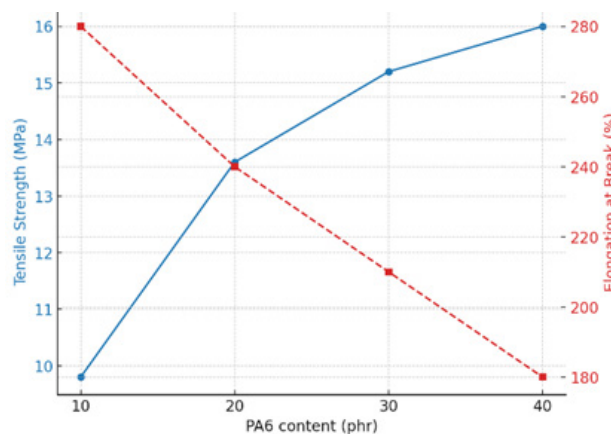


Figure 1 – Variation of tensile strength and elongation at break of EPDM/PA6 blends compatibilized with DCP as a function of PA6 content

When PA6 is added, stiffness increases, but the same tendency is observed for elastomer-thermoplastic systems when elasticity is compromised. The optimal balance between strength and elasticity is obtained at moderate concentrations (20–30 phr PA6), without loss of retention and expansion.

Figure 2 shows the effect of PA6 on the modulus and hardness of EPDM/PA6 blends.

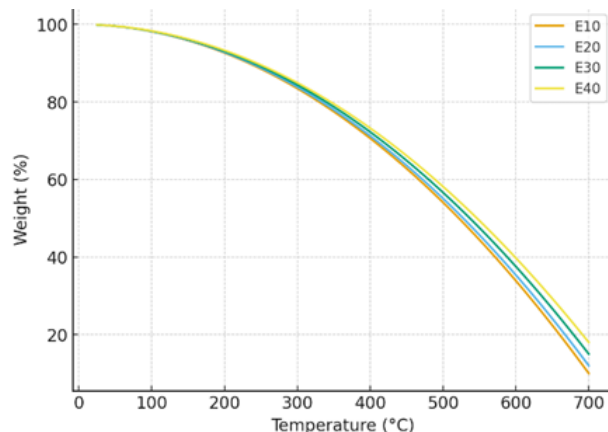


Figure 2 – Effect of PA6 loading on modulus and hardness of EPDM/PA6 blends

Both modulus and A-hardness increase in the same way with increasing PA6 concentration. Since PA6 domains act as rigid reinforcements, the resistance to deformation under tension in the blends increases. The transition from a soft elastomeric material to a harder elastomeric-thermoplastic is fully confirmed as the hardness increases. These results confirm the suitability of such blends for engineering applications where high stiffness resistance and dimensional stability are required, such as automotive parts and cable insulation.

As shown in Figure 3, the thermal decomposition of EPDM/PA6 blends strongly depends on the PA6 content. The shift of the TGA curves towards higher temperatures and the increasing residual yield are in full agreement with the data presented in Table 3 and confirm the increased thermal stability of blends with higher PA6 loading (Figure 4).

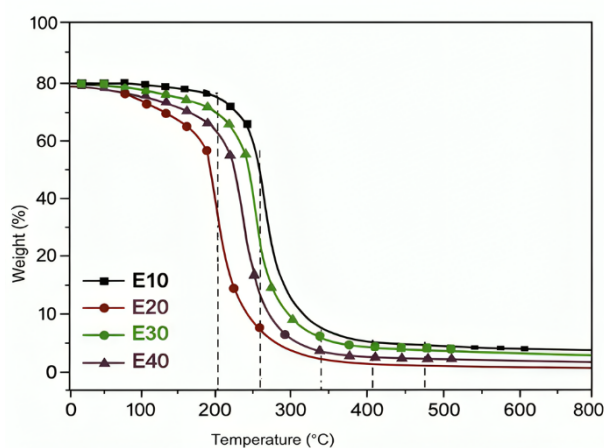


Figure 3 – TGA curves of EPDM/PA6 mixed with different PA6 compositions

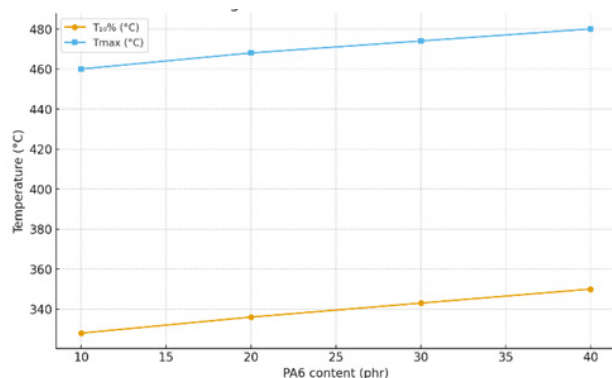


Figure 4 – Dependence of T_{max} from PA6 content in EPDM/PA6

Figure 5 shows the temperature variation of the storage modulus (E') for EPDM/PA6 blends due to the strengthening effect of PA6 as well as the adaptation by DCP.

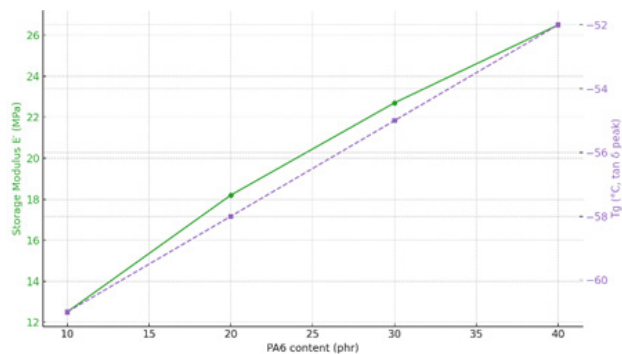


Figure 5 – Storage modulus (E') of EPDM/PA6 blends versus temperature, the stiffening effect of PA6 and the adaptation by DCP

The dynamic mechanical analysis results show that the storage modulus (E') increases steadily with PA6 loading. This confirms the increased stiffness and energy storage capacity. Also, the glass transition temperature (T_g , observed from the $\tan\delta$ peak) shifts upwards from -61°C to -52°C . At this time, stronger interfacial interactions reflect limited chain mobility. The decrease in $\tan\delta$ peak intensity and lower interfacial friction at higher PA6 levels indicate more efficient stress transfer between phases, which fully proves the effectiveness of peroxide-induced adaptation.

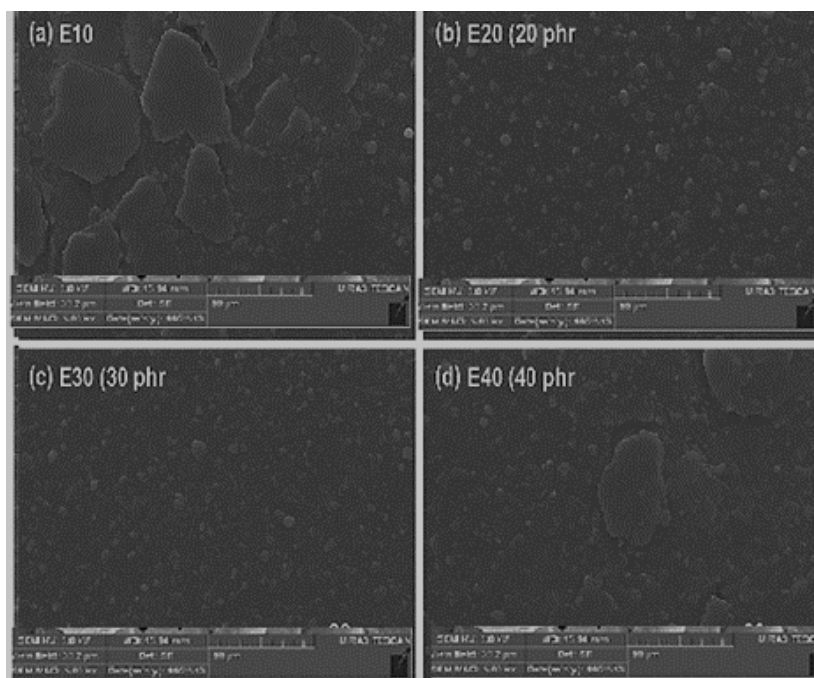
As shown in Figure 6, the SEM micrographs illustrate the fractured surface morphology of EPDM/PA6 blends, where samples E10, E20, E30, and E40 exhibit variations in dispersion and interfacial adhesion.

E10 (10 phr PA6): Large, irregular PA6 domains are clearly visible with distinct boundaries, reflecting poor interfacial adhesion. This morphology corresponds to moderate tensile strength and high elongation at break. Poor adhesion leads to voids and poor stress transfer in the thermoplastic phase dispersed from the EPDM matrix. As a result, the material exhibits a strong effect at low tensile strength, which maintains a high elongation at break, which mainly affects the toughness of the rubber.

E20 (20 phr PA6): According to the SEM images provided, it shows a fine morphology with smaller uniformly dispersed PA6 particles. The difference between the interfaces is less noticeable,

which indicates that the DCP-induced grafting reactions are good, indicating that the polar PA6 and non-polar EPDM phases are well matched.

This fine dispersion also results in high levels of strength and modulus while maintaining the existing elasticity.



(a) E10, (b) E20, (c) E30, and (d) E40

Figure 6 – High-magnification SEM micrographs of EPDM/PA6 blends

E30 (30 phr PA6): The most homogeneous morphology is achieved at this composition. PA6 particles are finely dispersed and well bonded to the EPDM matrix, resulting in excellent stress transfer and the best balance of stiffness and toughness [34]. The strong interfacial adhesion allows efficient stress transfer across the two phases, leading to the best overall balance of stiffness, toughness, and elongation. This explains why the E30 blend is identified as the optimal composition in terms of mechanical performance.

E40 (40 phr PA6): Agglomeration of PA6 domains reappears, leading to localized stress concentrations and premature fracture during deformation. This explains the reduced elongation at break despite further increases in tensile strength and hardness [29–32]. At high PA6 loadings, the micrographs reveal the reappearance of agglomerated PA6 clusters and microcracks around rigid particles. These features act as stress concentrators, which promote brittle fracture and reduce elongation at break, even though tensile strength and hardness continue to in-

crease. Thus, the excessive thermoplastic fraction undermines toughness and flexibility.

The SEM observations clearly demonstrate that 20–30 phr PA6 (E20–E30) offers the most favorable morphology, where PA6 domains are sufficiently small, uniformly dispersed, and well-bonded to the EPDM matrix due to DCP-induced compatibilization. This composition provides an optimal compromise:

- improved tensile strength and stiffness (due to effective reinforcement by PA6);
- maintained elasticity and toughness (due to the continuous rubbery EPDM phase);
- enhanced interfacial adhesion (due to peroxide-initiated grafting).

In contrast, 10 phr PA6 is insufficient to achieve meaningful reinforcement, while 40 phr PA6 causes phase agglomeration and embrittlement. Therefore, the 20–30 phr range is the most suitable ratio for engineering applications demanding a balance of mechanical strength, flexibility, and thermal stability.

Conclusion

In this study, EPDM/PA6 blends compatibilized with dicumyl peroxide (DCP) were systematically prepared and characterized in terms of mechanical, thermal, and morphological properties. The results collectively highlight the decisive role of PA6 content and peroxide-induced compatibilization in tailoring the performance of elastomer/thermoplastic systems.

The results of the tests showed that the inclusion of PA6 in the blends significantly increased the tensile strength, modulus of elasticity and hardness. This is explained by the reinforcing effect of the hard thermoplastic phases. Also, increasing the amount of PA6 showed a loss of elasticity, while simultaneously reducing the elongation at break. The optimum limit between strength and elasticity was achieved at 20–30 phr PA6; at these contents, the blends provided sufficient strength as well as acceptable elongation.

The results of the thermal analysis confirmed that PA6 improved the thermal stability of the blends. As the amount of PA6 increased, both the initial decomposition temperature ($T_{10\%}$) and the maximum decomposition temperature (T_{max}) gradually shifted towards higher values. This, together with the higher char residue observed at higher loadings, indicates a positive effect of the PA6 and DCP-induced adaptation on the overall thermal resistance of the blends.

Dynamic mechanical analysis confirmed the stiffening effect of PA6, showing a systematic increase in storage modulus and a shift of the glass transition temperature (T_g) towards higher values. These results reflect the strengthening of interfacial adhesion and the limitation of chain mobility. This is also attributed to peroxide-mediated grafting reactions at the EPDM/PA6 interface.

Morphological analysis by SEM directly demonstrated the effect of PA6 concentration on phase dispersion. At low PA6 content (E10), large and poorly bonded phase domains were observed, which is consistent with low strength and high elongation. At other PA6 proportions (E20–E30), finely dispersed and well-bonded PA6 particles were obtained, confirming effective tailoring. It also explained the superiority of mechanical properties. At high PA6 content (E40), however, microcracking of the particles was observed, which led to a decrease in impact strength despite an increase in tensile strength.

Overall, the findings demonstrate that DCP is an efficient reactive compatibilizer for EPDM/PA6 blends, enabling improved phase adhesion and tunable property profiles. The optimal formulations were identified at 20–30 phr PA6 with 1.0–1.2 phr DCP, providing the best trade-off between tensile strength, toughness, thermal stability, and morphological uniformity. These compositions are therefore promising for industrial applications—such as automotive parts, cable insulation, and structural components—where a balance of elasticity, strength, and heat resistance is critical.

The mechanical and thermal results obtained in this study are not only of laboratory interest but also highly relevant for industrial applications. In particular, the EPDM/PA6 blends containing 20–30 phr PA6, which demonstrated tensile strengths in the range of 13–15 MPa while maintaining adequate elasticity, are promising for automotive engineering components such as vibration-damping parts, heat- and oil-resistant seals in the engine compartment, and shock-absorbing elements.

The improvement in thermal stability, with the onset degradation temperature increasing from 328°C to 350°C, further indicates that these blends can be effectively employed in cable insulation materials and energy transport systems where elevated temperatures are encountered. Moreover, the enhanced modulus and hardness suggest their suitability for structural components requiring dimensional stability and durability under mechanical stress.

Therefore, scaling the mechanical and thermal findings to real-world applications clearly demonstrates that DCP-compatibilized EPDM/PA6 blends are not limited to fundamental research but offer significant potential in automotive, construction, and energy infrastructure sectors, where a combination of flexibility, mechanical robustness, and heat resistance is essential.

Acknowledgments

The authors gratefully acknowledge the support provided by Tekoplast Company.

Conflict of interest

The authors declare that they have no conflicts of interest.

References

1. Kumar R., et al. (2021) Mechanical performance and sustainability of polymer composites: A critical review. *Materials Science Forum*, 1012, pp.1. <https://doi.org/10.4028/www.scientific.net/MSF.1012.1>.
2. Movlayev I.G., Mammadova A.F. (2024) Determination of the main parameters of the modified epoxide oligomer. *Int. Sci. J. Eng. Agric.*, 3(6), pp. 95. <https://doi.org/10.46299/j.isjea.20240306.09>.
3. Amirli F.A., Movlayev I.H., Aliyeva G.A., Mammadova A.F. (2023) Compositions based on modified and filled epoxy oligomer. *Processes of Petrochemistry and Oil Refining*, 24(4), pp. 689. <https://doi.org/10.36719/1726-4685/96/689-696>.
4. Mammadov S., Mammadova G., Khankishiyeva R., Azizova G., Movlayev I., Mammadov J. (2023) The effect of composition and structure of NBR-based elastomer blends in the vulcanization process and study of their aging by exposure to heat and radiation. *Chemistry & Chemical Technology*, 17(4), pp. 829. <https://doi.org/10.23939/chcht17.04.829>.
5. Aghamaliyev Z.Z., Naghiyeva M.V., Rasulov Ch.K. (2018) Synthesis of 2-Hydroxy-3-(methylcyclohexenyl-isopropyl)-5-methylbenzylaminoethylonyl imidazolines as thermostabilizers to polypropylene. *Materials Science Forum*, 935, pp. 155. <https://doi.org/10.4028/www.scientific.net/MSF.935.155>.
6. Amirli F.A., Azizova G.G., Mammadova A.F., Irvanli K.B. (2025) Study of the features of vulcanization and the character of vulcanization structures of nitrile butadiene rubber. *Processes of Petrochemistry and Oil Refining*, Special issue, 2025, pp. 259-264. <https://doi.org/10.62972/1726-4685.si2025.1.259>.
7. Klyuchnikov O.R., Deberdeev R.Ya., Zaikov G.E. (2006) Low-temperature vulcanisation of unsaturated rubbers by C-nitrose systems. *International Polymer Science and Technology*, 3, pp. 51. <https://doi.org/10.1177/0307174X0603300810>.
8. Amirli F.A., Movlayev I.H., Mammadova A.F. (2025) Study of the rheological properties of the mixture of terminal ethylene-propylene rubber with benzenamine-modified phenol–formaldehyde oligomer. *Processes of Petrochemistry and Oil Refining*, 26(1), pp. 229–239. <https://doi.org/10.62972/1726-4685.2025.1.229>.
9. Dyshyn O., Habibov I., Suleymanova A., Abasova S., Malikov R., Khankishiyeva T. (2023) Identifying the mechanism of formation of a natural nanocomposite in polymer composite materials. *Eastern-European Journal of Enterprise Technologies*, 2(6-122), pp. 24. <https://doi.org/10.15587/1729-4061.2023.277587>.
10. Park G., Kim Y.-H., Kim D. S., et al. (2010) Morphology and vulcanizate properties of ethylene-propylene-diene rubber/styrene-butadiene rubber blends. *Journal of Nanoscience and Nanotechnology*, 10(5), pp. 3720. <https://doi.org/10.1166/jnn.2010.2348>.
11. Mammadov S., Mammadova G., Khankishiyeva R., Amirov F., Azizova G., Movlaev I., Mammadov J. (2023) Investigation of the rheological structural parameters of a network of NBR-based vulcanizates with the participation of chlorine-containing compounds. *Journal of New Technology and Materials*, 13(1), pp. 70.
12. Mammadov S., Mammadova G., Khankishiyeva R., Amirov F., Azizova G., Movlaev I., Mammadov J. (2023) Properties of vulcanizates based on nitrile butadiene rubber in the occurrence of halomethyl-containing compounds. *Functional Materials*, 30(3), pp. 393. <http://dx.doi.org/10.15407/fm30.03.393>.
13. Ibragimova M.C., Amirov F.A., Bayramova S.T. (2020) Investigation of reactivity of the petroleum polymer pitch on the basis of gasoil fraction. *Processes of Petrochemistry and Oil Refining*, 24(3), pp. 347.
14. Ma L., Yang W., Guo H. (2019) Effect of cross-linking degree of EPDM phase on the morphology evolution and crystallization behavior of thermoplastic vulcanizates based on polyamide 6 (PA6)/ethylene-propylene-diene rubber (EPDM) blends. *Polymers*, 11(9), pp. 1375. <https://doi.org/10.3390/polym11091375>.
15. Lin X., Li Y., Zhang Z., Liu J. (2020) Reactive compatibilization of polyamide 6 with olefin block copolymers: morphology, rheology and mechanical properties. *Polymers*, 12(5), pp. 1123. <https://doi.org/10.3390/polym12051123>.
16. Hel C.L., Smith A.B., Jones D.R. (2020) Thermoplastic vulcanizates: new insight on rubber morphology and phase behavior. *Polymers*, 12(10), pp. 2315. <https://doi.org/10.3390/polym12102315>.
17. Amirli F., Khankishiyeva R., Movlayev I., Mammadova A. (2025) Properties of NBR/modified EPDM rubber compositions. *Physics and Chemistry of Solid State*, 26(3), pp. 549-555. <https://doi.org/10.15330/pcss.26.3.549-555>.
18. Song L.F., Müller K., Becker M. (2023) Effects of ethylene-propylene-diene monomer characteristics on TPV performance and morphology. *Polymers*, 15(2), pp. 345. <https://doi.org/10.3390/polym15020345>.
19. Çakır N.Y., Wang S., Roberts I. (2023) Unlocking the potential use of reactive POSS as a compatibilizer and coagent in peroxide-cured TPVs. *Polymers*, 15(7), pp. 1489. <https://doi.org/10.3390/polym15071489>.
20. Piontek A., Vernaez O., Kabasci S. (2020) Compatibilization of poly(lactic acid) (PLA) and bio-based EPDM via reactive extrusion with different coagents. *Polymers*, 12(3), pp. 605. <https://doi.org/10.3390/polym12030605>.
21. Ma L., Guo H., Yang W. (2019) In-situ dynamic vulcanization and interfacial compatibilization in PA6/EPDM TPVs: effects on crystallization and mechanical performance. *Journal of Applied Polymer Science*, 136(14), pp. 47215.
22. Mirzaee R., Park S. (2020) Modeling and optimizing toughness and rigidity in PA6/SBR blends using experimental design and reactive compatibilization. *Polymer*, 188, pp. 122121. <https://doi.org/10.1016/j.polymer.2020.106346>.
23. Tang Q., Li Y., Zhou X. (2022) Morphological evolution and damping properties of dynamically vulcanized TPVs: role of curing degree and compatibilizer. *Materials*, 15(5), pp. 1789.
24. Ma L., Guo H. (2019) Effect of peroxide dosage on morphology and mechanical properties of PA6/EPDM blends. *Materials*, 12(18), pp. 2953.
25. Bhattacharya A.B., Fernández M. (2020) Automotive applications of thermoplastic vulcanizates: review and perspectives. *Polymer Reviews*, 60(4), pp. 585-612.
26. Mirzaee R., Zhao K. (2020) Optimizing compatibilizer type and loading for PA6/EPDM based blends: mechanics and morphology. *Polymer Engineering & Science*, 60(9), pp. 2030-2042.

29. Maity A., Naskar K., Bhowmick A.K. (2016) Peroxide-induced compatibilization in elastomer/thermoplastic blends: mechanism and processing. *Polymer International*, 65(11), pp. 1360-1374.
30. Li L., Zhang T. (2012) Characterization of PA6/EPDM-g-MA/HDPE ternary blends: phase morphology and mechanical performance. *Polymer*, 53(8), pp. 1702-1710.
31. Nakason C., Praserttham P. (2013) Thermoplastic natural rubber based on polyamide-12 and EPDM: morphology by reactive compatibilization. *Journal of Elastomers & Plastics*, 45(3), pp. 245-261.
32. Zhu L., Wang H. (2018) Core-shell morphology effects on mechanical properties in PA6/HDPE/compatibilizer systems. *Macromolecules*, 51(20), pp. 8202-8214.
33. Cui Z., Sun L. (2023) Effect of crosslinking agent dosage on the morphology and thermal stability of TPVs based on various rubbers. *Composites Part A: Applied Science and Manufacturing*, 164, pp. 106771.
34. Helms G., Noordermeer J. (2014) Peroxide-induced dynamic vulcanization and interfacial compatibilization methodologies: a review. *Biomacromolecules*, 15(6), pp. 2038-2052.

Information about authors:

Fariz Amirli – Professor, Doctor of Technical Sciences, Azerbaijan State Oil and Industry University (Baku, Azerbaijan, e-mail: fariz.amirli@asoiu.edu.az).

Rana Khankishiyeva – Doctor of Philosophy in Radiation Materials Science, Azerbaijan State Oil and Industry University; Institute of Radiation Problems; Azerbaijan University of Architecture and Construction; Scientific-Research Institute Geotechnological Problems of Oil, Gas and Chemistry (Baku, Azerbaijan, e-mail: rana.khankishiyeva@azmiu.edu.az).

Aynur Mammadova – PhD candidate, Azerbaijan State Oil and Industry University (Baku, Azerbaijan, e-mail: aynur.memmedova@asoiu.edu.az).

Samira Bayramova – Researcher, Azerbaijan State Oil and Industry University (Baku, Azerbaijan, e-mail: bayramova.samira.t@gmail.com).

Gunel Azizova – Researcher, Azerbaijan State Oil and Industry University (Baku, Azerbaijan, e-mail: azizova.gunel@asoiu.edu.az).

Konul Iranvanli – Researcher, Azerbaijan State Oil and Industry University (Baku, Azerbaijan, e-mail: iranvanli.konul@asoiu.edu.az).